Many-body properties of a spherical two-dimensional electron gas

J. Tempere,[1,2] I. F. Silvera,[1] and J. T. Devreese[2]
[1]*Lyman Laboratory of Physics, Harvard University, Cambridge, Massachusetts 02138*
[2]*Dept. Natuurkunde, Universiteit Antwerpen (UIA), Universiteitsplein 1, B2610 Antwerpen, Belgium*
(Received 5 November 2001; published 8 May 2002)

We investigate the many-body properties of a two-dimensional electron gas constrained to the surface of a sphere, a system which is physically realized in, for example, multielectron bubbles in liquid helium. A second-quantization formalism, suited for the treatment of a spherical two-dimensional electron gas (S2DEG), is introduced. Within this formalism, the dielectric response properties of the S2DEG are derived, and we identify both collective excitations and a spectrum of single-particle excitations. We find that the single-particle excitations are constrained to a well-defined region in the angular-momentum–energy plane. The collective excitations differ in two important aspects from those of a flat 2DEG: on a sphere, the ''spherical plasmons'' have a discrete frequency spectrum and the lowest frequency is nonzero.

DOI: 10.1103/PhysRevB.65.195418 PACS number(s): 73.20.−r, 05.30.Fk, 71.10.−w

I. INTRODUCTION

When a film of electrons on a flat helium surface reaches a critical density, the helium surface becomes unstable[1] and multielectron bubbles form.[2] These multielectron bubbles are spherical cavities in the helium liquid, containing from a few to several tens of millions of electrons. The bubble radius R is determined by balancing the Coulomb repulsion of the electrons in the bubble with the surface tension of the helium: for $N=10\,000$ electrons, the typical bubble radius is 1 μm, and scales as $N^{2/3}$.[3] Density functional calculations[4,5] indicate that the electrons inside the bubble are not spread out homogeneously, but instead form a thin spherical layer with thickness $\delta \ll R$ and radius $\approx R-\delta$, anchored to the surface of the helium, with a binding energy of the order of several kelvin.[4,6] The electrons are free to move in the directions tangential to the spherical helium surface, so that in effect they form a spherical two-dimensional electron gas (S2DEG).

Our present analysis of the spherical two-dimensional electron gas, albeit motivated by the study of multielectron bubbles, is equally relevant from a fundamental point of view: it is the logical next step to take after analysis of the flat two-dimensional electron gas, a topic that keeps drawing renewed attention. Furthermore, S2DEG's also appear in doped semiconductor particles if carriers accumulate in a surface layer,[7] in charged droplets,[8] and in fullerenes, where multipole excitation modes with angular momentum $l=1,2,3,4$ of the S2DEG have recently been investigated.[9]

In this paper, we introduce a second-quantization formalism suited for the description of the S2DEG (in Sec. II). On the basis of this formalism, the angular-momentum-dependent dielectric function of the S2DEG is derived within the random phase approximation (RPA) framework in Sec. III. Results are given for the single-particle and collective excitations of the S2DEG and the static structure factor dependence on the angular momentum quantum number in Sec. IV.

II. HAMILTONIAN OF THE S2DEG

Decompositions in plane waves $\varphi_{\mathbf{k}}(\mathbf{r}) \propto e^{i\mathbf{k}\cdot\mathbf{r}}$ are well suited to handle the many-body problem in flat space, but are not appropriate to describe the many-body problem on a spherical surface. The noninteracting single-particle wave functions suitable for the description of the S2DEG are spherical harmonics, $\varphi_{l,m}(\Omega)=Y_{l,m}(\Omega)$, where Ω represents the spherical angles $\Omega=\{\theta,\phi\}$, and l,m represent the angular momentum quantum numbers. We introduce the creation operator $\hat{c}^{\dagger}_{l,m}$ which creates an electron in the state $\varphi_{l,m}(\Omega)$ on the sphere if no electron is present in that state and the annihilation operator $\hat{c}_{l,m}$ which destroys an electron in the single-particle state $\varphi_{l,m}(\Omega)$.

A. Kinetic energy

Within second-quantization theory (see, e.g., Ref. 10), the kinetic energy operator can be written as a function of $\hat{c}^{\dagger}_{l,m}$ and $\hat{c}_{l,m}$ as follows:

$$\begin{aligned}\hat{T}=&\sum_{l=0}^{\infty}\sum_{m=-l}^{l}\sum_{l'=0}^{\infty}\sum_{m'=-l'}^{l'}\hat{c}^{\dagger}_{l,m}\\&\times\left[\int d\Omega\, Y^{*}_{l,m}(\Omega)\frac{-\hbar^2}{2m_eR^2}\Delta_{\Omega}Y_{l',m'}(\Omega)\right]\hat{c}_{l',m'}\\=&\sum_{l=0}^{\infty}\sum_{m=-l}^{l}\frac{\hbar^2 l(l+1)}{2m_eR^2}\,\hat{c}^{\dagger}_{l,m}\hat{c}_{l,m}.\end{aligned}\tag{1}$$

In this expression, m_e is the electron mass, R is the radius of the spherical electron gas, Δ_{Ω} is the angle-dependent part of the Lagrangian in spherical coordinates, and $\int d\Omega = \int_0^{2\pi} d\phi \int_0^{\pi} d\theta \sin\theta$. Expression (1) shows that the energy of a free electron in an angular momentum state $\{l,m\}$ is

$$E_{l,m}=\frac{\hbar^2 l(l+1)}{2m_eR^2}.\tag{2}$$

If more than one electron is present, they will occupy the lowest-energy states up to the Fermi energy E_F characterized by a Fermi angular momentum L_F, so that $N=2(L_F+1)^2$ and $E_F=\hbar^2 L_F(L_F+1)/(2m_eR^2)$. Since in multielectron bubbles the bubble radius $R\propto N^{2/3}$,[11] the Fermi energy scales

as $E_F \propto N^{-1/3}$ so that adding electrons to the multielectron bubbles lowers the Fermi energy.

B. Density

The surface density on the sphere, defined as the expectation value of the number of electrons in an infinitesimal spherical angle around Ω, is

$$\hat{n}_e(\Omega)=\sum_{l=0}^{\infty}\sum_{m=-l}^{l}\sum_{l'=0}^{\infty}\sum_{m'=-l'}^{l'} Y^*_{l,m}(\Omega)Y_{l',m'}(\Omega)\hat{c}^\dagger_{l,m}\hat{c}_{l',m'}. \tag{3}$$

The decomposition in spherical harmonics of this density operator is given by

$$\hat{n}_e(\Omega)=\sum_{l=0}^{\infty}\sum_{m=-l}^{l}\hat{\rho}_e(l,m)Y^*_{l,m}(\Omega), \tag{4}$$

$$\hat{\rho}_e(l,m)=\int d\Omega \hat{n}_e(\Omega)Y_{l,m}(\Omega). \tag{5}$$

Using the parity property of spherical harmonics, $Y_{l,m}(\Omega)=(-1)^m Y^*_{l,-m}(\Omega)$, it is easily shown that $\hat{\rho}_e(l,m)=(-1)^m\hat{\rho}_e(l,-m)$. Substituting Eq. (3) in Eq. (4), we find for the spherical components of the density operator

$$\hat{\rho}_e(l,m)=\sum_{l_1=0}^{\infty}\sum_{m_1=-l_1}^{l_1}\sum_{l_2=0}^{\infty}\sum_{m_2=-l_2}^{l_2}\times\left[\int d\Omega Y_{l,m}(\Omega)Y^*_{l_2,m_2}(\Omega)Y_{l_1,m_1}(\Omega)\right]\times\hat{c}^\dagger_{l_2,m_2}\hat{c}_{l_1,m_1}. \tag{6}$$

The addition rules for spherical harmonics allow us to perform the integral of the product of spherical harmonics in Eq. (6):

$$\hat{\rho}_e(l,m)=\sum_{l'=0}^{\infty}\sum_{m'=-l'}^{l'}\sum_{L=|l-l'|}^{l+l'}\sum_{M=-L}^{L}\sqrt{\frac{(2l+1)(2l'+1)}{(2L+1)}}\times\langle l,0;l',0|L,0\rangle\langle l,m;l',m'|L,M\rangle\hat{c}^\dagger_{L,M}\hat{c}_{l',m'}. \tag{7}$$

In this expression, $\langle l,m;l',m'|L,M\rangle$ is the Clebsch-Gordan coefficient for combining the angular momenta $\{l,m\}$ and $\{l',m'\}$ into $\{L,M\}$. To simplify this expression, we introduce the following notation:

$$\hat{c}^\dagger_{(l,m)\otimes(l',m')}=\sum_{L=|l-l'|}^{l+l'}\sum_{M=-L}^{L}\sqrt{\frac{(2l+1)(2l'+1)}{(2L+1)}}\times\langle l,0;l',0|L,0\rangle\langle l,m;l',m'|L,M\rangle\hat{c}^\dagger_{L,M}. \tag{8}$$

The operator $\hat{c}^\dagger_{(l,m)\otimes(l',m')}$ creates an electron in a state which results from the combination of two angular momentum states characterized by the quantum numbers $\{l,m\}$ and $\{l',m'\}$, respectively. With this notation, the spherical components of the density operator can be written as

$$\hat{\rho}_e(l,m)=\sum_{l'=0}^{\infty}\sum_{m'=-l'}^{l'}\hat{c}^\dagger_{(l,m)\otimes(l',m')}\hat{c}_{l',m'}, \tag{9}$$

which highlights the analogy with the definition of the Fourier-transformed density operator of the flat two-dimensional electron gas.

C. Coulomb interaction on the sphere

The Coulomb potential energy term for N electrons, in the Hamiltonian is

$$\hat{H}_{\text{Coulomb}}=\frac{1}{2}\sum_{j=1}^{N}\sum_{j'\neq j=1}^{N}\frac{e^2}{4\pi\varepsilon_0}\frac{1}{|\hat{\mathbf{r}}_j-\hat{\mathbf{r}}_{j'}|}, \tag{10}$$

where $\hat{\mathbf{r}}_j$ represents the position operator of electron j and ε_0 is the vacuum permittivity. The Coulomb potential on a sphere with radius R can be straightforwardly expanded in spherical harmonics:

$$\hat{H}_{\text{Coulomb}}=\frac{1}{2}\sum_{j=1}^{N}\sum_{j'\neq j=1}^{N}\frac{e^2}{4\pi\varepsilon R}\sum_{l=0}^{\infty}\sum_{m=-l}^{l}\frac{4\pi}{2l+1}\times Y_{l,m}(\hat{\Omega}_j)Y^*_{l,m}(\hat{\Omega}_{j'}), \tag{11}$$

with $\hat{\Omega}_j$ the (spherical angle) position operator of electron j on the sphere. In second quantization this becomes

$$\hat{H}_{\text{Coulomb}}=\sum_{l_1,m_1}\sum_{l_2,m_2}\sum_{l.m}(-1)^m v(l)\times\hat{c}^\dagger_{(l_1,m_1)\otimes(l,-m)}\hat{c}^\dagger_{(l_2,m_2)\otimes(l,m)}\hat{c}_{l_2,m_2}\hat{c}_{l_1,m_1}, \tag{12}$$

with $\Sigma_{l,m}=\Sigma_{l=0}^{\infty}\Sigma_{m=-l}^{l}$ and

$$v(l)=\frac{e^2}{2\varepsilon R}\frac{1}{2l+1}. \tag{13}$$

This term in the Hamiltonian describes the interaction process, shown in Fig. 1. The initial state consists of two electrons in angular momentum states $\{l_1,m_1\}$ and $\{l_2,m_2\}$. In the final state one electron is in an angular momentum state resulting from adding $\{l,m\}$ to its original angular momentum, and the other electron is in a state resulting from subtracting $\{l,m\}$ from its original angular momentum. Hence, the Coulomb interaction on a spherical surface can be described as the exchange of a virtual photon with a given angular momentum $\{l,m\}$, with an amplitude for this process of $v(l)$. The total Hamiltonian for the S2DEG is

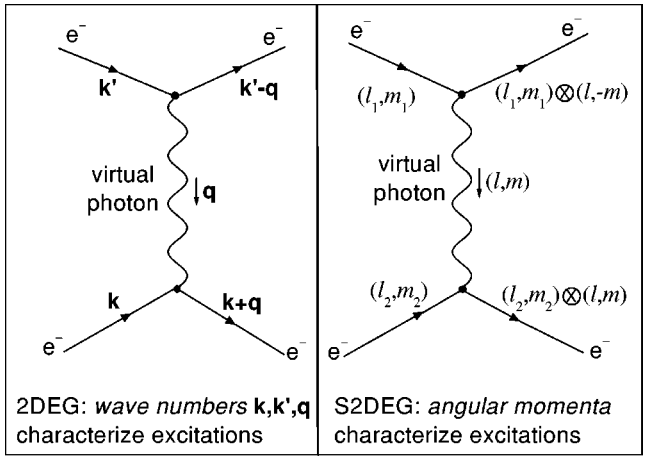

FIG. 1. Two Feynman diagrams for equivalent processes—namely, the exchange of a virtual photon between two electrons. The panel at the left shows the diagram for the case of a flat 2DEG and the one to the right is for the case of a S2DEG. In the flat 2DEG, wave numbers are good quantum numbers; in the S2DEG, they have to be replaced by angular momentum quantum numbers. Vector addition of momenta has to be replaced by addition of angular momenta.

$$\hat{H}=\sum_{l=0}^{\infty}\sum_{m=-l}^{l}\frac{\hbar^2 l(l+1)}{2m_e R^2}\hat{c}^{\dagger}_{l,m}\hat{c}_{l,m} + \sum_{l_1,m_1}\sum_{l_2,m_2}\sum_{l,m}(-1)^m v(l) \times \hat{c}^{\dagger}_{(l_1,m_1)\otimes(l,-m)}\hat{c}^{\dagger}_{(l_2,m_2)\otimes(l,m)}\hat{c}_{l_2,m_2}\hat{c}_{l_1,m_1}. \quad (14)$$

III. RESPONSE PROPERTIES OF THE S2DEG

When an external field $V_{\rm ext}(\Omega;\omega)=\Sigma_{l,m}V_{\rm ext}(l,m;\omega)Y_{l,m}(\Omega)$ that couples to the electron density is applied, an induced density $\rho_{\rm ind}(\Omega,\omega)=\Sigma_{l,m}\rho_{\rm ind}(l,m;\omega)Y_{l,m}(\Omega)$ is generated. Within linear response theory, the spherical components of this induced density can be written as

$$\rho_{\rm ind}(l,m;\omega)=\frac{1}{\hbar}V_{\rm ext}(l,m;\omega)\mathcal{D}_R(l,m;\omega), \quad (15)$$

where $\mathcal{D}_R(l,m;\omega)$ is the retarded density-density Green's function.[12] If the external potential $V_{\rm ext}(l,m;\omega)$ is a Coulomb potential created by an external charge $\rho_{\rm ext}$, a dielectric function depending on the angular momentum can be introduced to describe the screening of this external Coulomb potential:

$$\varepsilon(l,m;\omega)=1-\frac{\rho_{\rm ind}(l,m;\omega)}{\rho_{\rm ext}(l,m;\omega)} \quad (16)$$

$$\Rightarrow\frac{1}{\varepsilon(l,m;\omega)}=1+\frac{v(l)}{\hbar}\mathcal{D}_R(l,m;\omega). \quad (17)$$

The retarded Green's function $\mathcal{D}_R(l,m;\omega)$ is derived from the density-density Green's function:

$$\mathcal{D}(l,m;t)=-i\left\langle\Psi_0\left|\mathcal{T}\left\{\sum_{l_1,m_1}\hat{c}^{\dagger}_{(l,m)\otimes(l_1,m_1)}(t)\hat{c}_{l_1,m_1}(t) \times\sum_{l_2,m_2}(-1)\hat{c}^{\dagger}_{(l,-m)\otimes(l_2,m_2)}\hat{c}_{l_2,m_2}\right\}\right|\Psi_0\right\rangle, \quad (18)$$

where the expectation value is taken with respect to the many-body ground state $|\Psi_0\rangle$, $\mathcal{T}$ is the time-ordering operator, and

$$\hat{c}_{l,m}(t)=e^{i\hat{H}t/\hbar}\hat{c}_{l,m}e^{-i\hat{H}t/\hbar}. \quad (19)$$

Within the second-quantization formalism for the S2DEG, $\mathcal{D}_R(l,m;\omega)$ is evaluated with standard Green's function techniques. In the resulting Feynman graphs (the "polarization bubble" graphs,[13]) the wave numbers are replaced by angular momenta as illustrated in Fig. 1. To lowest order in the interaction amplitude $v(l)$, we find

$$\mathcal{D}_R^{(0)}(l,m;\omega)=\sum_{l',m'}\sum_{L=|l-l'|}^{l+l'}\frac{(2l+1)(2l'+1)}{4\pi(2L+1)}n(l',m')[1-n(L,m+m')]|\langle l,0;l',0|L,0\rangle|^2|\langle l,m;l',m'|L,m+m'\rangle|^2 \times\left(\frac{1}{\omega+(E_{l',m'}-E_{L,m+m'})/\hbar+i\eta}-\frac{1}{\omega+(E_{L,m+m'}-E_{l',m'})/\hbar+i\eta}\right), \quad (20)$$

with η an infinitesimal number; $E_{l,m}$ the energy of a free electron in angular momentum state $\{l,m\}$ on the sphere, and

$$n(l,m)=\langle\Psi_0|\hat{c}^{\dagger}_{l,m}\hat{c}_{l,m}|\Psi_0\rangle, \quad (21)$$

the occupation number of state $\{l,m\}$. This result, derived with the formalism described in Sec. II, is in agreement with the result of Inaoka[9] for the susceptibility of the S2DEG, which was used to investigate the $l=1,2,3,4$ multipole modes of the S2DEG.[9] In Sec. IV we extend this investigation to include excitations with large angular momentum l (so that $l/L_F>1$), keeping the regime studied by Inaoka as a limiting case. By investigating a much broader portion of the excitation spectrum, we identify the nature of the excitations and expose novel properties of those excitations.

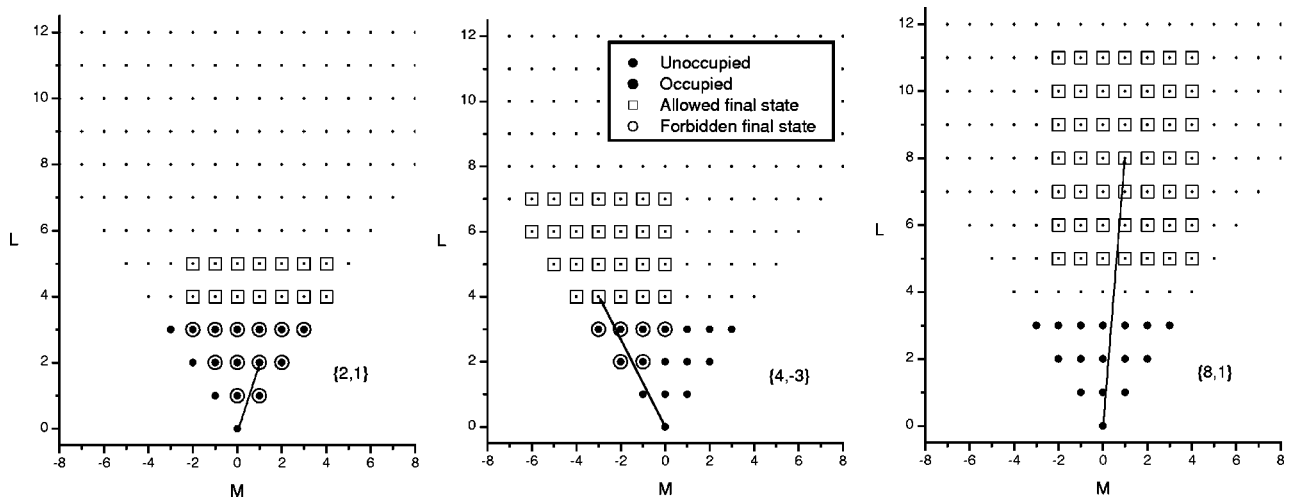

FIG. 2. Diagrams representing the angular momentum states of an electron on a spherical surface. In the three panels, electrons are occupying the single-particle states up to a Fermi-level angular momentum $L_F=3$. This Fermi sea of occupied states is shown as solid circles. The diagrams also show the final states which can occur from combining the angular momentum of any of the electrons in the Fermi sea with the angular momentum of an excitation (with $\{l,m\}=\{2,1\},\{4,-3\},\{8,1\}$ for the left, middle, and right panels, respectively). The final states which are unoccupied, and thus allowed, are indicated by open squares. The final states which cannot be achieved because there is already an electron present are indicated by open circles.

The contribution of lowest order in $v(l)$ to the retarded density-density Green's function determines the Hartree-Fock (HF) approximation to the dielectric function (17), given here for reference:

$$\varepsilon_{\mathrm{HF}}(l,m;\omega)=\left[1+\frac{v(l)}{\hbar}\mathcal{D}_R^{(0)}(l,m;\omega)\right]^{-1}. \tag{22}$$

It also permits the calculation of the RPA to the dielectric function, through a Dyson series for $\mathcal{D}_R^{\mathrm{RPA}}$:

$$\mathcal{D}_R^{\mathrm{RPA}}=\frac{\mathcal{D}_R^{(0)}}{1-[v(l)/\hbar]\mathcal{D}_R^{(0)}}, \tag{23}$$

so that

$$\varepsilon_{\mathrm{RPA}}(l,m;\omega)=1-\frac{v(l)}{\hbar}\mathcal{D}_R^{(0)}(l,m;\omega). \tag{24}$$

Note that the spin degree of freedom is not explicitly taken into account in the expressions above. The interparticle potential and the kinetic energy are considered to be spin-independent in the present treatment. The central quantity, from which properties of the S2DEG are derived in the current treatment, is the "polarization bubble" diagram leading to $\mathcal{D}_R^{(0)}$. For spin-independent interaction potentials, the spin degree of freedom only leads to a degeneracy prefactor $\mathcal{D}_R^{(0)}$: the degeneracy of the unperturbed levels is doubled from $2l+1$ to $2(2l+1)$.

IV. RESULTS AND DISCUSSION

A. Single-particle excitations

In this section we will use units such that $m_e=\hbar=R=1$. The dielectric function can be clarified by considering Plemelj's rule. The imaginary part of the RPA dielectric function becomes

$$\begin{aligned}\mathrm{Im}\varepsilon_{\mathrm{RPA}}(l,m;\omega)=\pi v(l)\sum_{l'm'}\sum_{L=|l-l'|}^{l+l'}&\frac{(2l+1)(2l'+1)}{4\pi(2L+1)}\\&\times n(l'm')[1-n(L,m+m')]\\&\times|\langle l,0;l',0|L,0\rangle|^2\\&\times|\langle l,m;l',m'|L,m+m'\rangle|^2\\&\times\delta[\omega-(E_{L,m+m'}-E_{l',m'})].\end{aligned} \tag{25}$$

The dynamic structure factor of the S2DEG is related to the dielectric function by

$$\begin{aligned}S(l,m;\omega)&=-\frac{1}{\pi v(l)}\mathrm{Im}\left[\frac{1}{\varepsilon(l,m;w)}\right] \qquad (26)\\&=-\frac{1}{\pi v(l)}\frac{\mathrm{Im}[\varepsilon(l,m;\omega)]}{\{\mathrm{Re}[\varepsilon(l,m;\omega)]\}^2+\{\mathrm{Im}[\varepsilon(l,m;\omega)]\}^2}, \qquad (27)\end{aligned}$$

and can be interpreted as the probability that an excitation with given angular momentum quantum number $\{l,m\}$ and energy $\hbar\omega$ can be created. $S(l,m;\omega)$ is a quantity accessible to experiment, in particular scattering experiments. From expression (25) we conclude that $\mathrm{Im}\varepsilon_{\mathrm{RPA}}(l,m;\omega)$ is zero unless adding the angular momentum $\{l,m\}$ and the energy $\hbar\omega$ to

the ground state of the S2DEG can excite a single electron from an occupied state $[n(l',m')=1]$ into an unoccupied state $[n(L,m+m')=0]$. These are the single-particle excitations (called the ''Landau continuum'' in the case of the flat 2DEG). Figure 2 illustrates this concept in relation to the S2DEG. Three regimes can be distinguished.

(i) *Case 1.* $l<L_F$. In the left panel of Fig. 2, we show the case of angular momentum $\{l,m\}=\{2,1\}$ imparted on the system. The solid disks represent the occupied states, the open squares are allowed final states which can be reached by adding the angular momentum $\{l,m\}$ to the angular momentum of an electron in the Fermi sphere, and the open circles are forbidden final states as they are occupied and excluded by Fermi statistics. In this example the Fermi sea is filled up to $L_F=3$. Not all final states are accessible, since to excite an electron it has to go into a final state which is unoccupied (the open squares). This means in practice that the electrons which can participate in creating an excitation of angular momentum $\{l,m\}$ are the ones close to the Fermi level (in fact, those from level L_F-l up to L_F).

(ii) *Case 2.* $2L_F>l>L_F$. This is shown in the middle panel of Fig. 2 depicting single-particle excitations which have angular momentum $\{4,-3\}$. Now all the electrons in the Fermi sea can participate, but not all resulting final states are unoccupied.

(iii) *Case 3.* $l>2L_F$. An example is shown in the right graph of Fig. 2, for single-particle excitations of angular momentum $\{8,1\}$. Now not only can all electrons participate in the process, but also all possible final states are unoccupied and thus accessible.

The maximum energy difference between initial and final single-particle states in Fig. 2 is

$$\omega_{\max}(l)=\frac{\hbar^2}{2m_eR^2}[(L_F+l)(L_F+l+1)-(L_F)(L_F+1)]$$

$$=\frac{\hbar^2}{2m_eR^2}[l^2+l(2L_F+1)]. \tag{28}$$

The smallest energy difference in case 3 ($l>2L_F$) is

$$\omega_{\min}(l)=\frac{\hbar^2}{2m_eR^2}[(l-L_F)(l-L_F+1)-(L_F)(L_F+1)]$$

$$=\frac{\hbar^2}{2m_eR^2}[l^2-l(2L_F-1)-2L_F]. \tag{29}$$

The two frequencies $\omega_{\min}(l)$ and $\omega_{\max}(l)$ demarcate a region in the frequency versus angular momentum plane in which the single-particle excitations lie. Figure 3 shows the location of the excitations of the spherical two-dimensional electron gas in the angular momentum l versus frequency ω plane. The $\{l,\omega\}$ values corresponding to a single-particle excitation for an S2DEG with $L_F=10$ are shown in Fig. 3 as markers within the limiting frequencies $\omega_{\min}$ and $\omega_{\max}$ of the Landau continuum region shown by solid curves.

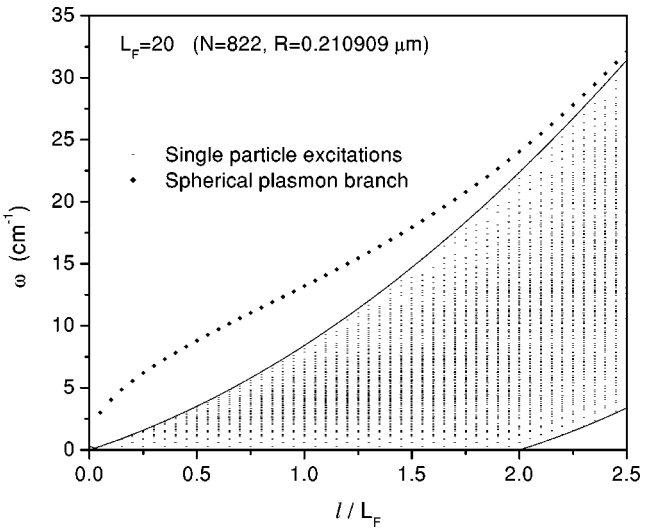

FIG. 3. In the many-body S2DEG, two types of excitations can be distinguished: single-particle excitations (which appear for $\mathrm{Im}[\varepsilon]\neq 0$) and collective excitations (which appear when $\mathrm{Re}[\varepsilon]=\mathrm{Im}[\varepsilon]=0$). The excitations of the S2DEG can be characterized by their angular momentum l and energy $\hbar\omega$. This figure shows the location of the excitations in the frequency (energy) vs angular momentum plane. The single-particle excitations are discrete, and all lie in a region demarcated by the black curves, representing $\omega_{\min}(l)$ and $\omega_{\max}(l)$ given by expressions (29) and (28). The collective excitations are shown as solid diamonds, lying above the $\omega_{\max}(l)$ curve.

B. Plasmons in a spherical 2D electron gas

In addition to the single-particle excitations in the S2DEG, collective excitations are also possible. ''Collective excitations'' are defined as poles of the density-density Green's function $\mathcal{D}$, whereas single-particle excitations are defined as poles of the single-particle Green's function.[12] This means that collective excitations appear when $\varepsilon(l,m;\omega)=0$. In the flat 2DEG, these collective excitations are called plasmon modes. We will use the same terminology for the S2DEG (occasionally using ''spherical plasmons'' when a distinction is needed).

For the collective mode, the imparted angular momentum is shared between all the particles. This means that in a collective mode with angular momentum $\{l,m\}$ the entire spherical shell of electrons will oscillate with an amplitude proportional to $Y_{l,m}(\Omega)$. The frequency of the collective modes (the plasma frequency ω_{pl}) will depend on the angular momentum of the mode $\{l,m\}$. The plasma frequency $\omega_{\mathrm{pl}}(l,m)$ of the S2DEG can be found by solving

$$1-\frac{e^2}{2\varepsilon\hbar R}\frac{1}{2l+1}\mathrm{Re}[\mathcal{D}_{R,0}(l,m;\omega_{\mathrm{pl}})]=0,$$

$$\mathrm{Im}[\mathcal{D}_{R,0}(l,m;\omega_{\mathrm{pl}})]=0. \tag{30}$$

For the flat electron gas the last condition means that the plasma branch lies outside the region of single-particle excitations discussed in the previous subsection. In Fig. 3, the spherical plasmon excitations are shown as full diamonds. Figure 4 illustrates how the plasmon branch depends on the

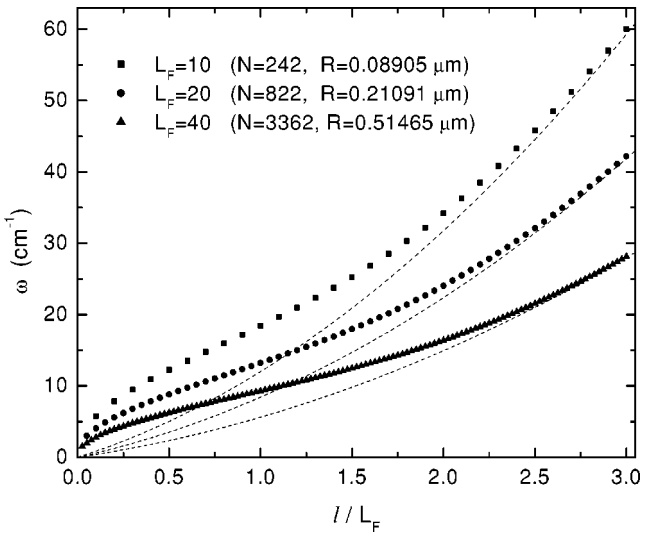

FIG. 4. The collective excitations of the S2DEG are the analog of plasmons in the flat 2DEG and appear at frequencies ω and angular momenta l such that $\mathrm{Re}[\varepsilon(l,\omega)]=\mathrm{Im}[\varepsilon(l,\omega)]=0$. For S2DEG's with $L_F=10,20,40$, these collective excitations are shown as solid squares, circles, and triangles, respectively. The dashed curves denote the upper frequency of the region of single-particle excitations [given by expression (28)]. As more electrons are put into the multielectron bubble, the frequency of the collective excitations decrease. As the Fermi level is increased, $L_F\rightarrow\infty$, the spherical plasmon excitations form a solid curve and the lowest spherical plasmon frequency $\omega_{\mathrm{pl}}(l=1)$ approaches zero.

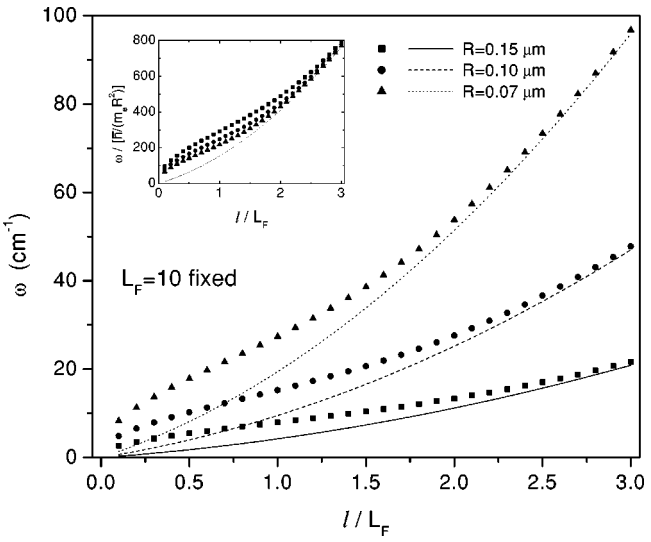

FIG. 5. In a multielectron bubble (MEB), the radius of the spherical electron gas can be varied independently of the number of electrons by applying pressure. This figure, which complements Fig. 4, shows the effect of changing the MEB radius on the frequencies of the collective excitations (the "spherical plasmons") as a function of the angular momentum. The inset shows the same results, with the frequency rescaled to the natural bubble frequency $\hbar/(m_eR^2)$.

number of electrons in the S2DEG. The radius of the S2DEG has been chosen equal to the equilibrium radius of a multielectron bubble with a given number of electrons.[11] The bubble radius is found by balancing the helium surface tension and the Coulomb repulsion as discussed in the introduction. Figure 5 illustrates how the plasmon branch depends on the radius of the S2DEG, for a fixed number of electrons. We find that as the radius is decreased (i.e., the multielectron bubble is compressed), the plasmon branch lies relatively closer to the upper frequency of the single-particle excitation region (as shown in the inset of Fig. 5). However, the energy scale, set by $\hbar^2/(m_eR^2)$, increases with decreasing radius so that the absolute value of the plasmon frequencies increases with decreasing radius. The plasmon frequency is independent of the projection of the angular momentum m. The plasmon branch of the S2DEG strongly differs from the plasmon branch of 2DEG's in two important aspects: it is discrete and the lowest accessible plasmon frequency is larger than zero despite the acoustic nature of the plasmon branch.

C. Sum rule and spectral weights

Sum rules prove to be a remarkably useful tool in the analysis of spectra, both experimentally and theoretically. The zeroth-moment sum rule for the dynamic structure factor defines the static structure factor $S(l,m)$:

$$S(l,m)=\int_0^\infty S(l,m;\omega)d\omega=-\frac{1}{\pi v(l)}\int_0^\infty \mathrm{Im}\left[\frac{1}{\varepsilon(l,m;\omega)}\right]d\omega. \tag{31}$$

Since the dynamic structure factor only depends on the magnitude of the angular momentum l and not on m, this will also be true for the static structure factor. Figure 6 shows the static structure factor as a function of angular momentum l. The open squares are the result in the Hartree-Fock approximation [using $\varepsilon_{\mathrm{HF}}$, expression (22)], and the solid circles are the result in the RPA approximation [using $\varepsilon_{\mathrm{RPA}}$, expression (24)]. As in the case of the flat 2DEG, the HF structure factor $S_{\mathrm{HF}}(l)$ is linear for small l/L_F, whereas the RPA structure factor approaches zero more rapidly with decreasing l. In the inset of Fig. 6, the first frequency moment of the dynamic structure factor,

$$\langle\omega(l)\rangle=\int_0^\infty \omega S(l,m;\omega)d\omega, \tag{32}$$

is shown, again for both HF and RPA approximations. Inaoka[9] derived a sum rule for the first frequency moment of the angular-momentum-dependent dynamic structure factor. In units $\hbar=m_e=R$, this is

$$\langle\omega(l)\rangle=\frac{l(l+1)}{2}. \tag{33}$$

From Fig. 6 it is clear that the HF dynamic structure factor obeys this sum rule. The RPA dynamic structure factor can be written as a sum of a contribution from the plasmon mode and the contribution S_{cont} from single-particle excitations:

$$S_{\mathrm{RPA}}(l;\omega)=A(l)\,\delta[\omega-\omega_{\mathrm{pl}}(l)]+S_{\mathrm{cont}}(l;\omega), \tag{34}$$

with $A(l)$ the spectral weight of the plasmon branch. The inset of Fig. 6 shows $\int\omega S_{\mathrm{cont}}(l,\omega)d\omega$. From the deficit of

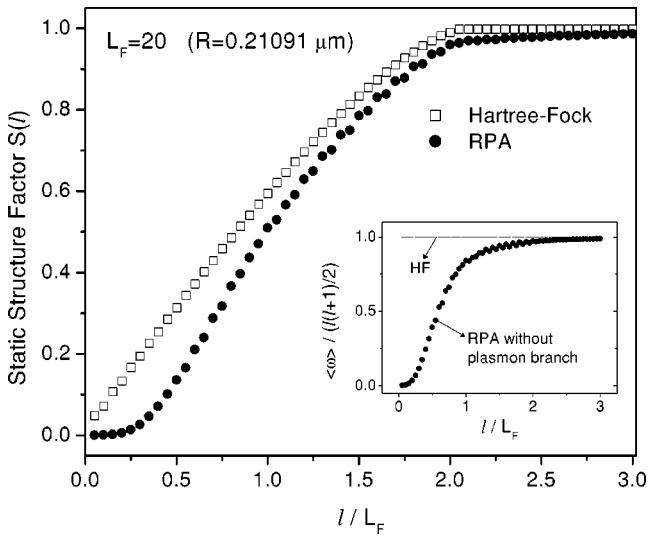

FIG. 6. The static structure factor $S(l)$ for a spherical two-dimensional electron gas (S2DEG) with $L_F=20$ is shown as a function of l, both in the RPA and in the Hartree-Fock approximations. Note that in the Hartree-Fock approximation, $S(l)$ is linear in l at small l, whereas in the RPA approximation it goes to zero faster than linearly. In the inset, the sum rule (33) for the first frequency moment of the dynamic structure factor of the S2DEG (Ref. 9) is checked. The Hartree-Fock result complies perfectly to the sum rule. The RPA result without the plasmon branch does not have enough spectral weight to satisfy the sum rule for $l/L_F<2$, which indicates that in this region a substantial part of the spectral weight lies with the plasmon mode—the strength of the plasmon branch is derived from this result.

the RPA dynamic structure factor without the plasmon mode, shown in the inset of Fig. 6, the spectral weight of the plasmon mode can be derived:

$$A(l)\omega_{\rm pl}(l)=\frac{l(l+1)}{2}-\int_0^\infty \omega S_{\rm cont}(l,\omega)d\omega. \qquad (35)$$

The spectral weight of the plasmon mode, along with the RPA dynamic structure factor in the region of single-particle excitations, is shown in Fig. 7 for $L_F=20$. The RPA dynamic structure factor of the S2DEG is shown color coded and as a function of the angular momentum l and the energy $\hbar\omega$. In white regions the RPA dynamic structure factor is zero. In shaded regions, the RPA dynamic structure factor differs from zero. This figure is the complement of Fig. 3: whereas Fig. 3 shows the location and type of the possible excitations of the S2DEG as a function of angular momentum and energy, this figure shows their corresponding spectral weight as expressed by the dynamic structure factor. At small angular momentum ($l/L_F<0.5$), the plasmon branch carries the most spectral weight, and the region of single-particle excitations only has a small fraction of the total spectral weight. Within the region of single-particle excitations, there is a local maximum in the dynamic structure factor around $l=L_{\rm F}$.

D. Discussion

The dynamic structure factor $S(l,m;\omega)$ is the spectral function of the density-density Green's function and as such can be interpreted as a probability function (see, e.g., Ref. 13, p. 153). Here $S(l,m;\omega)d\omega$ is the probability that an excitation of the S2DEG has angular momentum quantum numbers $\{l,m\}$ and energy between $\hbar\omega$ and $\hbar(\omega+d\omega)$. This is analogous to the interpretation of the more familiar dynamic structure factor $[S(\mathbf{k},\omega)]$ expressed as a function of wave number, which is the probability that an excitation has momentum $\hbar\mathbf{k}$ and energy $\hbar\omega$.

A "natural" experiment to determine the dynamic structure factor directly is an inelastic scattering experiment. In particular the differential cross section for a probe particle of mass M (such as an incident ion) and initial momentum $\mathbf{p}_{\rm i}$ to be scattered to a final state $\mathbf{p}_{\rm F}$ with energy transfer between $\hbar\omega$ and $\hbar(\omega+d\omega)$ to the scattering system is[12]

$$\frac{d\sigma}{d\theta d\omega}=\frac{M^2}{8\pi^3}\frac{p_f}{p_i}|V_k|^2S(k,\omega). \qquad (36)$$

In this expression, θ is the scattering angle between $\mathbf{p}_{\rm f}$ and $\mathbf{p}_{\rm i}$, $|V_{\mathbf{k}}|$ is the Fourier transform of the interaction potential between the probe particle, and the energy transfer ω is related to the momentum transfer $\mathbf{k}$ by $\hbar\omega=\hbar^2\mathbf{k}\cdot\mathbf{p}_{\rm i}/m+(\hbar k)^2/(2m)$. The relation between the Fourier decomposition and the spherical decomposition of the density is

$$\hat{\rho}_{\rm e}(\mathbf{k})=\sum_{j=1}^{N}\langle e^{i\mathbf{k}\cdot\hat{\mathbf{r}}_j}\rangle=\sum_{j=1}^{N}\sum_{l}\sqrt{4\pi(2l+1)}i^l j_l(kR)\langle Y_{l,0}(\hat{\theta}_j)\rangle$$

$$=\sum_{l}\sqrt{4\pi(2l+1)}i^l j_l(kR)\hat{\rho}_{\rm e}(l,0), \qquad (37)$$

where the z axis has been taken along the direction of the wave vector $\mathbf{k}$, $j_l(x)$ is the spherical Bessel function of the first kind, and θ_j is the angle between $\mathbf{k}$ and the position operator of electron $j,\mathbf{r}_j$. The dynamic structure factors are related by

$$S(k,\omega)=\sum_{l}|\sqrt{4\pi(2l+1)}j_l(kR)|^2S(l,0;\omega), \qquad (38)$$

which can be derived by writing the dynamic structure factor as a density-density correlation function in the Lehmann representation and substituting expression (37) for $\hat{\rho}_{\rm e}(\mathbf{k})$.

Note that the dependence of the angular wave functions on the polar angle θ becomes semiclassical when the quantum number l is large. In particular, the WKB expression for the angular function becomes[14]

$$Y_{l0}(\theta)\approx\frac{i^l}{\pi}\frac{\sin[(l+1/2)\theta+\pi/4]}{\sqrt{\sin\theta}}. \qquad (39)$$

This semiclassical approximation will be valid in the region where $\theta l\gg 1$ and $(\pi-\theta)l\gg 1$, which holds at large l for almost all values of θ except those close to the "poles" $\theta=0$ and $\theta=\pi$. The semiclassical approximation (39) corresponds to the limit of a plane wave, where the wavelength is given by $R(2\pi/l)$. As such, this approximation leads primarily to the results of a flat 2D electron gas where $\hbar l/R$ plays the role of the electron momentum. This is valid in the limit

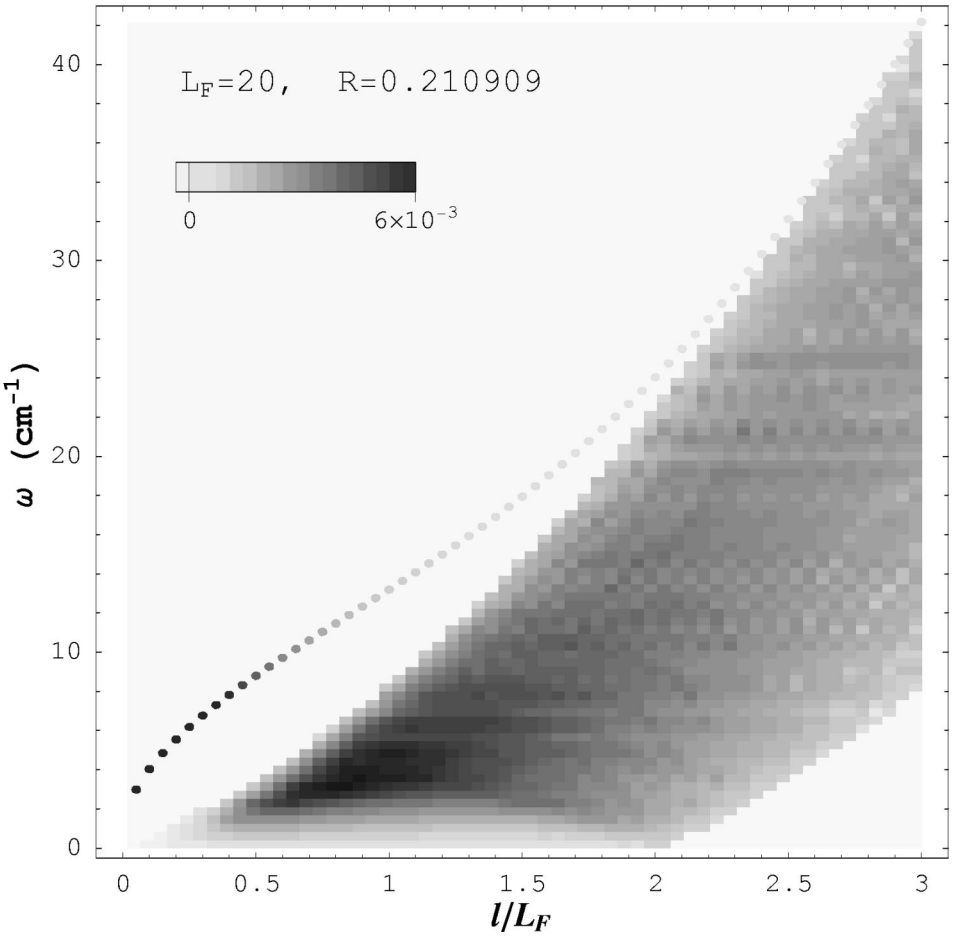

FIG. 7. The RPA dynamic structure factor $S(l,\omega)$ for a spherical two-dimensional electron gas (S2DEG) with $L_F=20$ is shown here in units $\hbar=m_e=R=1$ as a function of the angular momentum quantum number l and their energy ω. At zero temperature, the RPA dynamic structure factor of the S2DEG consists of a region of single-particle excitations and a set of collective modes (colored disks). This figure complements Fig. 3, which shows only the locations of the excitations, whereas this figure shows their spectral weights.

that R is large and the ratio l/R remains finite, although even for small R, this approximation will still hold at large l. However, it does not reproduce some of the interesting low-angular-momentum results such as a lower boundary to the plasmon frequencies.

V. CONCLUSIONS

In this paper, we have studied the properties of the two-dimensional electron gas in a distinct geometry which is recently gaining interest in connection to multielectron bubbles—namely, electrons confined to a spherical surface. For this purpose, we set up a second-quantization formulation based on the spherical harmonics as single-electron building blocks for the many-electron theory, introduced in Sec. II. Within this formalism, the dynamic structure factor is derived in the RPA framework and both the single-particle excitations and collective excitations are analyzed for S2DEGs with L_F up to 40 and for angular momenta l up to $3L_F$.

The dynamic structure factor in the RPA approximation reveals collective excitations (''spherical plasmon modes''), which differ from the collective modes of the flat 2DEG in that the spherical plasmon modes of the S2DEG are discrete in frequency and the smallest spherical plasmon frequency is larger than zero. For $l/L_F<0.5$, we find that the spherical plasmon mode carries the main fraction of the spectral weight. The single-particle excitations are confined to a region determined by $\omega_{\min}(l)$ and $\omega_{\max}(l)$ given by expressions (29) and (28). In the semiclassical approximation, the role of the electron momentum $\hbar k$ in the flat 2DEG is played by $\hbar l/R$ in the spherical electron gas, and the energy scale is set by $\hbar^2/(m_eR^2)$, which opens interesting prospects for multielectron bubbles since the radius can be varied by either changing the number of electrons or—independently—the pressure. For typical multielectron bubbles with $N\leqslant 10^4$, the plasmon modes of the S2DEG lie in the far infrared, and their frequency increases with decreasing number of electrons in the multielectron bubble or with decreasing radius of the bubble, such that these novel collective modes may be detectable in forthcoming experiments on stabilized multielectron bubbles.[15]

ACKNOWLEDGMENTS

Discussions with V. Fomin, S. Klimin, and J. Huang are gratefully acknowledged. J. T. is supported financially by the FWO-Flanders. This research has been supported by the Department of Energy and by the GOA BOF UA 2000, IUAP, and FWO-V Project Nos. G.0071.98, G.0306.00, G.0274.01, WOG WO.025.99N (Belgium).

[1] L.P. Gor'kov and D.M. Chernikova, JETP Lett. **18**, 68 (1973).
[2] A.P. Volodin, M.S. Khaikin, and V.S. Edel'man, Pis'ma Zh. Éksp. Teor. Fiz. **26**, 707 (1977) [JETP Lett. **26**, 543 (1977)]; U. Albrecht and P. Leiderer, Europhys. Lett. **3**, 705 (1987).
[3] V.B. Shikin, JETP Lett. **27**, 39 (1978).
[4] M.M. Salomaa and G.A. Williams, Phys. Rev. Lett. **47**, 1730 (1981).
[5] K.W.K. Shung and F.L. Lin, Phys. Rev. B **45**, 7491 (1992).
[6] M.W. Cole, Rev. Mod. Phys. **46**, 451 (1974).
[7] Y. Sasaki, Y. Nishina, M. Sato, and K. Okamura, Phys. Rev. B **40**, 1762 (1989).
[8] J.W. Rayleigh, Philos. Mag. **14**, 184 (1882).
[9] T. Inaoka, Surf. Sci. **273**, 191 (1992).
[10] S. S. Schweber, *An Introduction to Relativistic Quantum Field Theory* (Row-Peterson, Evanston, Illinois, 1961).
[11] V.B. Shikin, Sov. Phys. JETP **33**, 387 (1971); **34**, 1095 (1972).
[12] D. Pines, *The Many-Body Problem* (Benjamin, New York, 1961).
[13] G. Mahan, *Many-Particle Physics* (Plenum, New York, 1993).
[14] L. F. Landau and E. M. Lifshitz, *Quantum Mechanics: Non-Relativistic Theory* (Pergamon, New York, 1977), para. 49.
[15] I.F. Silvera, Bull. Am. Phys. Soc. **46**, 1016 (2001).